Analysis of the Material Removal Rate and Smoothing Effect of Active Fluid Jet Polishing

Vipender Singh Negi[1,2*], Harry Garg[1,2], Shravan Kumar R R[2], Vinod Karar[2], Umesh Kumar Tiwari[1,2]
1. Academy of Scientific and Innovative Research (AcSIR), CSIR-CSIO Campus, Chandigarh, India
2. CSIR-Central Scientific Instruments Organisation, Chandigarh, India
[*]Corresponding author: vipender@live.com

Abstract
Active fluid jet polishing is a sub-aperture polishing process used in the optical fabrication of complex surfaces. Finishing and correction of surface irregularities during the polishing process is challenging. Quality of optical surface depends on smoothing action during fine and correction polishing. In this paper, polishing analysis of active fluid jet polishing is discussed. In, active fluid jet polishing, the polishing compound stream is used to press a cylindrical tip against the optical surface. Polishing action is created by polishing fluid, pressure, and relative velocity of the carrier placed at the end of the cylindrical tip. During the polishing process, a tool influence function is convoluted along the polishing path to uniformly polish the surface. The optical surface material removal rate during polishing depends on contact pressure, relative velocity, properties of the polishing slurry, carrier, and workpiece. A mathematical model describing the kinematic and pressure distribution is described. Effect of pressure, spot size and tool speed on the material removal rate and surface irregularities are discussed.

Keywords: Asphere, Finishing, Polishing, Sub-aperture

Introduction

Optical polishing is the computer controlled polishing process used during optical fabrication. Different types of components include flat, lens and mirrors. The optical component can be classified into axisymmetric and non-axisymmetric surfaces[1,2]. Challenges increase during the fabrication of non-axisymmetric surfaces. For imaging optical application the quality of surface topography[3] is comparable to operational wavelength (sub-wavelength for figure and in nanometer/sub-nanometer range for surface roughness).
The objective of the polishing process is to create a specular smooth surface, fine adjust the figure, and improve surface finish. sub-aperture polishing is used for zonal polishing of the complex surface. The polishing process is carried in steps from pre-polishing, correction, and fine polishing. The high material removal rate is required during the pre-polishing process and a lower material removal rate is preferred during correction polishing to reduce the sensitivity of the correction process. Sub-aperture pad polishing tool can be classified in terms of rigidity, i.e. rigid[4], semi-rigid and flexible tool. The rigid tool provides natural smoothing and flexible tool deflects according to the contacting surface. Other important polishing and finishing processes include fluid jet polishing[5], magneto rheological finishing[6], and ion beam finishing. During polishing, there are inherent tool signature[7] generated due to tool motion during grinding and pre-polishing process. For accurate optical surface, the optical surface requires low mid- to high-spatial frequency errors for imaging applications[8]. Optical quality in terms of contrast and resolution is based on optical fabrication quality.
Some of the important application areas where optical fabrication quality is required are medical imaging, surveillance systems, space telescopes, head up and head-mounted display systems, and lithography.
Although previous researchers attempted to solve the problem of surface quality, however, repeatability and accurate finishing of all class of optical components are still challenging due to stringent optical tolerances. Analysis of material removal rate (MRR) and smoothing process using active fluid jet polishing is presented in the paper. Different process parameters are considered for the investigations including tool speed, contact pressure, spot size. The smoothing process is investigated using the polishing of surface with known periodic irregularities.

Active Fluid Jet Polishing (AFJP)

AFJP is a polishing tool used in computer controlled optical surfacing. AFJP is a sub-aperture fine and correction polishing process (use for simple to complex optical surfaces). The polishing process using AFJP is based on fluid jet polishing, where a cylindrical pin with a polishing matrix on the front tip is placed inside a cylindrical cavity in the polishing nozzle. Pressurized fluid is feed from the cavity behind the cylindrical tip. This fluid presses the cylindrical tip against the glass surface. Fluid comes out from the annular spacing around the cylindrical polishing tip during tool rotation. The polishing tool is rotated about

the tool rotation axis. This creates eccentric motion (d) of the polishing spot. Eccentric motion helps in removing surface errors efficiently.

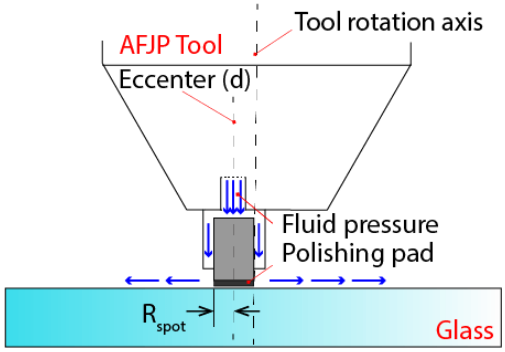

Figure 1. Active fluid jet polishing (AFJP) process (MCP 250 OptoTech).

The interaction diagram representing contact between AFJP tool and a flat workpiece is shown in Figure 1.

Numerical Model

Numerical modeling of the material removal rate of AFJP is described using Figure 2. Often during smoothing using the AFJP workpiece is rotated about the center axis passing through the workpiece center (O). Whereas the AFJP tool is rotated about the tool center (C).

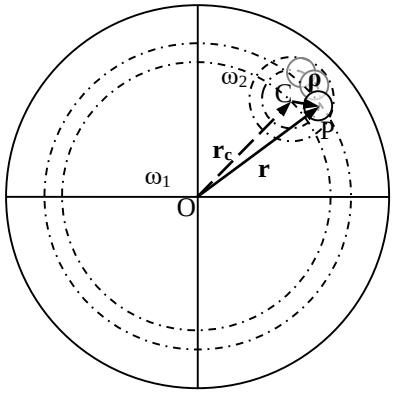

Figure 2. Kinematics of active fluid jet polishing.

Where ω_1 and ω_2 are the angular velocities of workpiece and tool respectively. For analysis, the workpiece is kept stationary and ω_2 is rotated about the tool axis. Tool center coordinate ($\mathbf{r_c}$) is defined by tool position. The position of spot center is defined by the radius vector ($\boldsymbol{\rho}$) whose magnitude depends on the eccentric distance (d). Figure 2. Shows the line diagram of the kinematics AFJP position.

The material removal rate (MRR) during polishing is described by Preston's equation (1). According to it, the rate of change of material removal depth is directly proportional to the pressure and relative velocity between the contacting surface.

$$R = \frac{dz}{dt} = \mathrm{kPV} \tag{1}$$

$$R(x,y) = -\frac{1}{\tau}\int_0^{\tau} kP_o e^{\left(-\frac{1}{2}\frac{(x_p-x_c)^2+(y_p-y_c)^2}{\sigma^2}\right)} v_{tw}(x,y)\, dt$$

Where R(x,y) is the average MRR, P_o is peak pressure (Gaussian distribution). $V_{tw}(x,y)$ is the relative velocity of the tool and k is Preston's coefficient. Aspheric equation (2) is widely used, due to several advantages of aspheric, it is used for defining optical surface including lens and the mirrors. For the analysis of the material removal rate and smoothing effect, the workpiece is assumed to be at rest and flat. The temperature, polishing process conditions are assumed to be constant. Preston's coefficient was determined experimentally.

$$z = \frac{cy^2}{1+\sqrt{1-(1+K)c^2y^2}} + \sum_{i=0}^{i=n} A_i y^i \tag{2}$$

In the aspheric equation, z is sagittal height, y radial distance from lens center, c is curvature, K is conic constant and A_i is the asphere coefficient. The polishing process is controlled using the dwell time. While polishing, the tool is pressed against the workpiece surface and polishing slurry is supplied near the contact zone. This creates a tool influence function (TIF). TIF is convoluted along the tool path to polish the surface. ODE and DAEs interfaces (3) in the Mathematical module in Comsol Multiphysics 5.4 was used for the polishing analysis. The analysis was carried using flat Schott BK7 glass (70 mm diameter).

$$e_a \frac{\partial^2 u}{\partial t^2} + d_a \frac{\partial u}{\partial t} = f \tag{3}$$

e_a is the mass coefficient, d_a is the damping coefficient and f is the source term taken from Preston's equation, where $e_a = 0$ and $d_a = 1$.

Initial value and time derivate of u (displacement)

$$u = 0 \text{ , and } \frac{du}{dt} = 0 \tag{4}$$

Position vector (5) of point P in Figure 2.

$$r = r_c + \rho \tag{5}$$

Process parameters used during analysis are tabulated in Table 1 below.

Table 1. AFJP polishing process parameters

Variable	Value			Units
Pressure (P_o)	1 to 1.5			bar
Tool speed (N_{ec})	500 to 2000			rpm
Spot radius (R_{spot})	2	3	5	mm
Eccenter (d)	0.5	1.5	2	mm

Results

Results during polishing are obtained by moving tools from edge to center. Figure 3. Shows the analysis of MRRs with different tool speeds and pressures. MRR increases with an increase in tool and peak pressure. The tool is moved from edge to center in 10 min duration, with spot radius 3 mm and eccentric distance 1.5 mm. The cross-section of removed material in a linear path at 1 bar is shown in Figure 4.

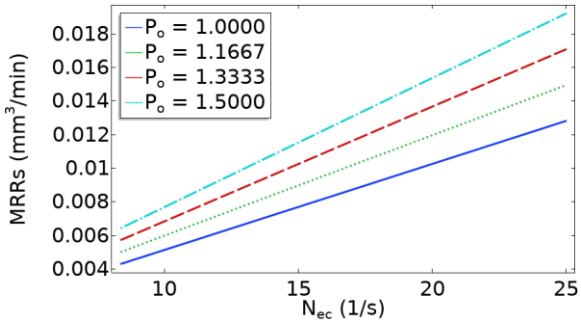

Figure 3. MRRs with varying tool rpm and peak pressure at 3 mm (R_{spot}).

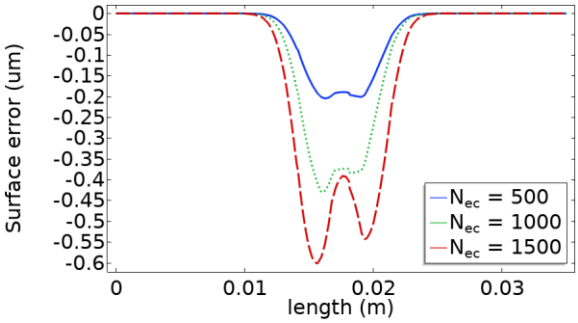

Figure 4. Removal depth at 1 bar, 3 mm (R_{spot}) and 600 s.

At high tool speed, the shape of the tool influence function deviated from pulse shape due to excessive material removal rate and can be observed in Figure 4 at 1500 rpm.

Another analysis for different spot radius was also carried. The material removal rate for different spot radius is shown in Figure 5. Three different spot radius 2 mm, 3 mm, and 5 mm were selected with the respective eccentric distance of 0.5 mm, 1.5 mm and 2 mm. It can be depicted from Figure 5, MRR increases markedly with an increase in spot size. Therefore spot radius can be used for controlling the polishing process efficiently.

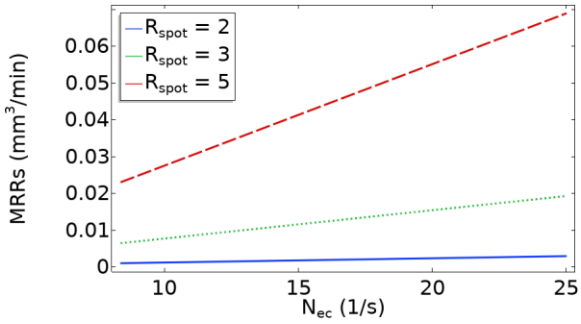

Figure 5. MRRs with different spot size at 1.5 bar.

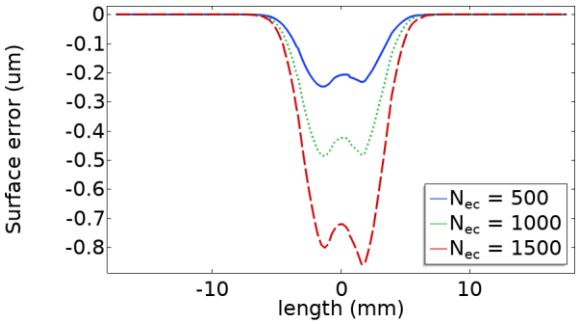

Figure 6. Removal depth at 1.5 bar, 3 mm (R_{spot}) and 600 s.

Similar to previous analysis the sectional profile of removed material is shown in Figure 6. The polishing was carried at 1.5 bar pressure higher than in Figure 4. With the increase in pressure material removal depth increases. The analysis was carried using 3 mm spot radius and 1.5 mm eccentricity for 10 min.

Analysis of the smoothing effect of AFJP was carried by the polishing of the sinusoidal periodic surface pattern. Figure 7 (left) shows the periodic surface pattern along the horizontal direction.

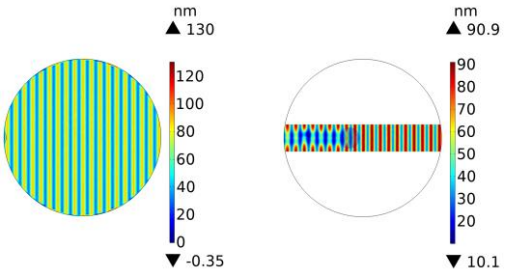

Figure 7. Initial generated sinusoidal surface error (left) and simulated surface error (Right) at 120 s, 1.5 bar, and 3 mm (R_{spot}).

The polishing process was carried with a 3 mm spot size, 1.5 bar pressure. AFJP tool was moved from the left edge to the center of the workpiece as shown in Figure 7 (Right).

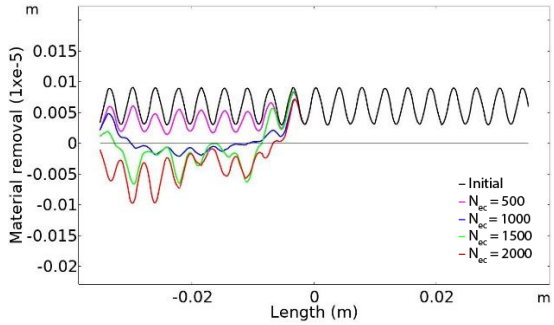

Figure 8. Section in contour at y = 0 (Figure 7, Right), smoothing using AFJP tool, 120 s, 1.5 bar, 3 mm (R_{spot}).

Figure 8. Shows the cross-sectional profile of a polished surface and it can be observed from Figure 7 (Right) and its cross-sectional profile (y = 0) in Figure 8, that amplitude of the irregularities is decreasing at low tool rpm but with further increase in the speed of tool, error amplitude is increasing in opposite direction.

Conclusions

1. AFJP can be used to obtain submicron or nanometer scale MRRs.
2. Due to low MRRs of the AFJP process, AFJP can be employed in fine and correction polishing.
3. AFJP can be employed in removing mid and high-spatial frequency surface errors on the optical surface during sub-aperture polishing.

References

1. Jain VK, Sidpara A, Balasubramaniam R, et al. Micromanufacturing: A review-Part I. *Proceedings of the Institution of Mechanical Engineers Part B-Journal of Engineering Manufacture*, **228**, 973-994 (2014)
2. Jones RA. Fabrication of small nonsymmetrical aspheric surfaces. *Applied Optics*, **18**, 1244-1246 (1979)
3. Archard JF. Contact and Rubbing of Flat Surfaces. *Journal of Applied Physics*, **24**, 981-988 (1953)
4. Kim DW and Burge JH. Rigid conformal polishing tool using non-linear visco-elastic effect. *Optics Express*, **18**, 2242-2257 (2010)
5. Fang H, Guo P and Yu J. Surface roughness and material removal in fluid jet polishing. *Applied Optics*, **45**, 4012-4019 (2006)
6. Dong ZC, Cheng HB and Tam HY. Modified dwell time optimization model and its applications in subaperture polishing. *Applied Optics*, **53**, 3213-3224 (2014)
7. Kim DW and Kim S-W. Static tool influence function for fabrication simulation of hexagonal mirror segments for extremely large telescopes. *Optics Express*, **13**, 910-917 (2005)
8. Hoyo JD, Choi H, Burge JH, et al. Experimental power spectral density analysis for mid- to high-spatial frequency surface error control. *Applied Optics*, **56**, 5258-5267 (2017)

Acknowledgements

The authors acknowledge their colleagues from CSIR-CSIO, Chandigarh, who provided the necessary resources, insight, and expertise that greatly assisted the research.